

Regulation of the collagen cross-linking enzymes *LOXL2* and *PLOD2* by tumor-suppressive *microRNA-26a/b* in renal cell carcinoma

AKIRA KUROZUMI^{1,2*}, MAYUKO KATO^{1,2*}, YUSUKE GOTO^{1,2}, RYOSUKE MATSUSHITA³,
RIKA NISHIKAWA^{1,2}, ATSUSHI OKATO^{1,2}, ICHIRO FUKUMOTO¹, TOMOHIKO ICHIKAWA² and NAOHIKO SEKI¹

Departments of ¹Functional Genomics and ²Urology, Chiba University Graduate School of Medicine, Chiba 260-8670;
³Department of Urology, Graduate School of Medical and Dental Sciences, Kagoshima University, Kagoshima 890-8520, Japan

Received January 25, 2016; Accepted February 22, 2016

DOI: 10.3892/ijo.2016.3440

Abstract. Our recent studies of microRNA (miRNA) expression signatures in human cancers revealed that *microRNA-26a* (*miRNA-26a*) and *microRNA-26b* (*miRNA-26b*) were significantly reduced in cancer tissues. To date, few reports have provided functional analyses of *miR-26a* or *miR-26b* in renal cell carcinoma (RCC). The aim of the present study was to investigate the functional significance of *miR-26a* and *miR-26b* in RCC and to identify novel *miR-26a/b*-mediated cancer pathways and target genes involved in RCC oncogenesis and metastasis. Downregulation of *miR-26a* or *miR-26b* was confirmed in RCC clinical specimens. Restoration of *miR-26a* or *miR-26b* in RCC cell lines (786-O and A498) revealed that these miRNAs significantly inhibited cancer cell migration and invasion. Our *in silico* analysis and luciferase reporter assays showed that lysyl oxidase-like 2 (*LOXL2*) and procollagen-lysine, 2-oxoglutarate 5-dioxygenase 2 (*PLOD2*) were directly regulated by these miRNAs. Moreover, downregulating the *PLOD2* gene significantly inhibited cell migration and invasion in RCC cells. Thus, our data showed that two genes promoting metastasis, *LOXL2* and *PLOD2*, were epigenetically regulated by tumor-suppressive microRNAs, *miR-26a* and *miR-26b*, providing important insights into the molecular mechanisms of RCC metastasis.

Introduction

Renal cell carcinoma (RCC) is a disease in which cells in the kidney tubules undergo oncogenic transformation. RCC has multiple subtypes and may occur in hereditary (2-3% of RCC) or sporadic forms (1,2). RCC is the third most common urolog-

ical cancer and accounts for 3% of all adult neoplasias. Clear cell RCC (ccRCC) is the most common subtype of sporadic RCC (~80%) (1). The standard curative treatment for localized diseases remains surgical excision with total nephrectomy. In contrast, at diagnosis, ~30% of RCCs have already metastasized. The 5-year survival rate in patients with advanced stage RCC is poor (5-10%) due to recurrence or distant metastasis (3,4). Recent molecularly targeted therapy has improved the survival rate of patients with advanced RCC (5,6). However, almost all patients eventually relapse or show distant metastasis due to acquired resistance to molecularly targeted therapy. Identifying molecular pathways responsible for RCC metastasis could provide novel approaches for the development of therapies that block the RCC metastatic pathways.

The discovery of microRNA (miRNA) in the human genome provided new directions in cancer research. The miRNAs are endogenous small RNA molecules (19-22 bases long) that regulate protein coding gene expression by repressing translation or cleaving RNA transcripts in a sequence-specific manner (7,8). Numerous studies have shown that miRNAs are aberrantly expressed in many human cancers, and they have significant roles in the initiation, development and metastasis of those cancers (9-11). Moreover, normal regulatory mechanisms can be disrupted by the aberrant expression of tumor-suppressive or oncogenic miRNAs in cancer cells. Therefore, identifying aberrantly expressed miRNAs is an important first step toward elucidating miRNA-mediated oncogenic pathways.

Using miRNA expression signatures, we have identified molecular pathways in RCC that are mediated by aberrantly expressed miRNAs (12-15). For example, downregulation of tumor-suppressive miR-218 promoted cancer cell migration and invasion through dysregulation of the focal adhesion pathway. In this regard, caveolin-2 has an oncogenic function in RCC cells (13). The epithelial-mesenchymal transition (EMT)-related *miR-200* family (*miR-200a/b/c*, *miR-141* and *miR-429*) is significantly downregulated in RCC where they act as tumor suppressors that target the focal adhesion and ErbB signaling pathways (14). The *miR-143/145* cluster was frequently reduced in RCC tissues; restoration of these miRNAs significantly inhibited RCC cell proliferation and invasion through targeting of hexokinase-2 (16). More recently, expression of the *miR-23b/27b* cluster was significantly decreased in ccRCC

Correspondence to: Dr Naohiko Seki, Department of Functional Genomics, Chiba University Graduate School of Medicine, 1-8-1 Inohana Chuo-ku, Chiba 260-8670, Japan
E-mail: naoseki@faculty.chiba-u.jp

*Contributed equally

Key words: *LOXL2*, microRNA, *miR-26a*, *miR-26b*, *PLOD2*, renal cell carcinoma

Table I. Characteristics of ccRCC clinical specimens.

No.	Pathology	Grade	pT	INF	v	ly	eg or ig	fc	im	rc	rp	s
1	Clear cell	G2	T1a	a	0	0	eg	1	0	0	0	0
2	Clear cell	G1>G2	T1a	a	0	0	eg	1	0	0	0	0
3	Clear cell	G3>G2	T1b	a	0	0	eg	1	0	0	0	0
4	Clear cell	G2>G3>G1	T1a	a	0	0	eg	1	0	0	0	0
5	Clear cell	G2>G3	T1b	a	0	0	eg	1	1	0	0	0
6	Clear cell	G2>G3	T3a	a	1	0	eg	1	0	0	0	0
7	Clear cell	G2>G3>G1	T3a	b	1	0	ig	0	1	1	0	0
8	Clear cell	G2>G3>G1	T3a	b	1	0	ig	1	0	0	0	0
9	Clear cell	G3	T3a	b	1	0	ig	0	0	0	0	0
10	Clear cell	G1>G2	T1b	a	0	0	eg	1	0	0	0	0
11	Clear cell	G2>G1>G3	T3a	b	1	0	ig	0	0	0	0	0
12	Clear cell	G2	T1a	a	0	0	eg	0	0	0	0	0
13	Clear cell	G2>G1>>G3	T1b	b	0	0	eg	1	0	0	0	0
14	Clear cell	G2>G1	T1a	b	0	0	eg	1	0	0	0	0
15	Clear cell	G2	T1b	a	0	0	eg	0	0	0	0	0

INF, infiltration; v, vein; ly, lymph node; eg, expansive growth; ig, infiltrative growth; fc, capsular formation; im, intrarenal metastasis; rc, renal capsule invasion; rp, pelvis invasion; s, sinus invasion.

tissues and associated with pathological grade and stage of the disease (17).

Our miRNA expression signatures of human cancers revealed that *miR-26a* and *miR-26b* were frequently downregulated in various types of cancer tissues (10,18,19), suggesting that these miRNAs act as tumor suppressors targeting several oncogenic pathways. Database searches revealed that there were few reports of functional analyses of *miR-26a* or *miR-26b* in RCC. The aim of the present study was to investigate the functional significance of *miR-26a* and *miR-26b* and to identify molecular targets and pathways contributing to metastasis in RCC cells by *miR-26a* or *miR-26b* regulation. We expect that this analysis will provide important insights into the potential molecular mechanisms of RCC oncogenesis and metastasis and will facilitate the development of therapeutic strategies for the treatment of the disease.

Materials and methods

RCC clinical specimens and cell culture. A total of 15 pairs of ccRCC specimens and corresponding non-cancerous specimens were collected from patients who had undergone radical nephrectomy at Chiba University Hospital (Chiba, Japan) from 2012 to 2015. These specimens were staged according to the General Rule for Clinical and Pathological Studies on Renal Cell Carcinoma based on the American Joint Committee on Cancer (AJCC)-UICC TNM classification. The clinicopathological characteristics of the patients are summarized in Table I. Before tissue collection, written informed consent of tissue donation for research purposes was obtained from all the patients.

We used two human RCC cell lines (786-O and A498) obtained from the American Type Culture Collection (ATCC; Manassas, VA, USA) as previously described (12-14).

Quantitative real-time reverse transcription polymerase chain reaction (qRT-PCR). The procedure for PCR quantification was previously described. TaqMan probes and primers for *LOXL2* (P/N: Hs00158757_ml; Applied Biosystems, Foster City, CA, USA), *PLOD2* (P/N: Hs01118190_ml; Applied Biosystems) and *GUSB* (the internal control; P/N: Hs00939627_ml; Applied Biosystems) were assay-on-demand gene expression products. The expression levels of *miR-26a* (assay ID: 000405; Applied Biosystems) and *miR-26b* (assay ID: 000407; Applied Biosystems) were analyzed by TaqMan quantitative real-time RT-PCR (TaqMan MicroRNA assay; Applied Biosystems) and normalized to the expression of RNU48 as previously described (12,20,21).

Transfection with mature miRNAs and siRNAs. The following mature miRNAs were used: Ambion Pre-miR miRNA precursor for *hsa-miR-26a-5p* (product ID: PM10249; Applied Biosystems) and for *hsa-miR-26b-5p* (product ID: PM12899; Applied Biosystems). The following siRNAs were used: Stealth Select RNAi si-RNA, *si-PLOD2* (cat nos. HSS108124 and HSS182371; Invitrogen) and negative control miRNA/siRNA (P/N: AM17111; Applied Biosystems). RNAs were incubated with Opti-MEM (Invitrogen) and Lipofectamine RNAiMax transfection reagent (Invitrogen) as previously described (12,20,21).

Cell proliferation, migration and invasion assays. 786-O and A498 cells were transfected with 10 nM miRNAs or si-RNAs by reverse transfection. Cell proliferation, migration and invasion assays were performed as previously described (12,20,21).

Western blotting. Cells were harvested 72 h after transfection, and lysates were prepared. Protein lysates (20 μ g) were separated on Mini-PROTEAN TGX gels (Bio-Rad Laboratories,

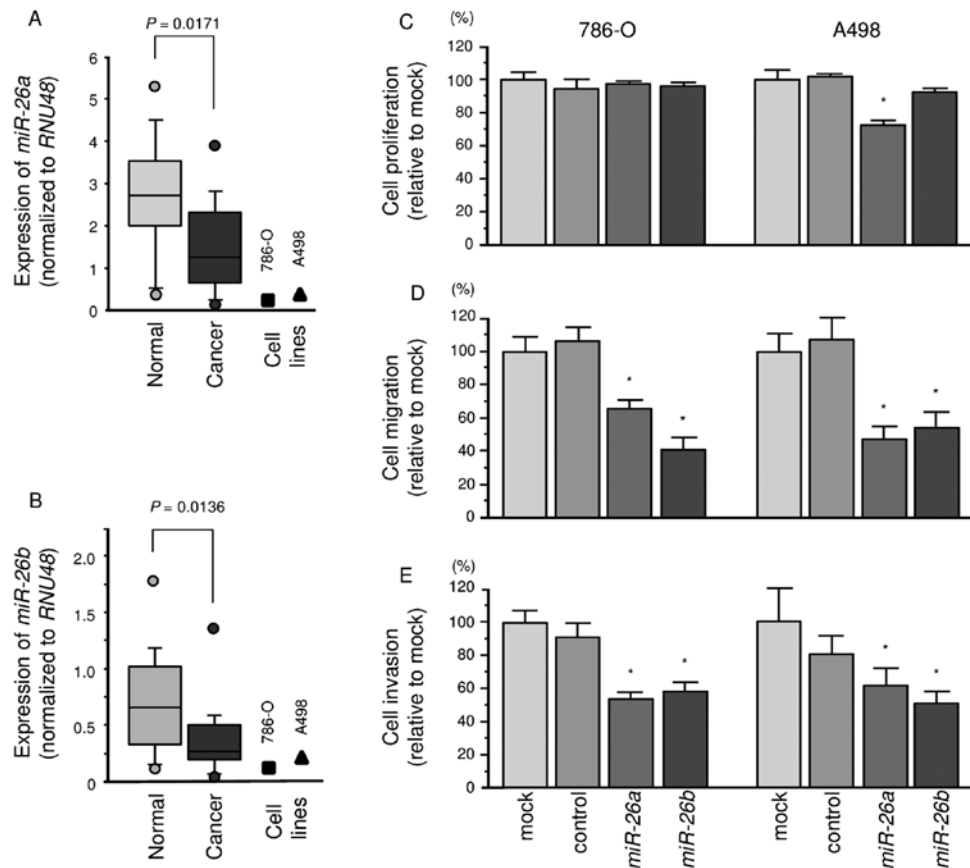


Figure 1. Expression levels of *miR-26a* and *miR-26b* in ccRCC clinical specimens and cell lines 786-O and A498. (A and B) Quantitative real-time RT-PCR showed that the expression levels of *miR-26a* and *miR-26b* were significantly lower in ccRCC tissues and RCC cell lines than in normal kidney tissues. *RNU48* was used as an internal control. (C-E) Effects of *miR-26a* or *miR-26b* transfection on RCC cell lines 786-O and A498. (C) Cell proliferation was determined by XTT assays 72 h after transfection with *miR-26a* or *miR-26b* (10 nM). (D) Cell migration activity was determined by wound-healing assays 48 h after transfection with *miR-26a* or *miR-26b* (10 nM). (E) Cell invasion activity was determined by Matrigel invasion assays 48 h after transfection with *miR-26a* or *miR-26b* (10 nM). * $P < 0.001$.

Hercules, CA, USA) and transferred to PVDF membranes. Immunoblotting was performed with rabbit anti-LOXL2 antibodies (1:1000; ab96233; Abcam, Cambridge, UK) and rabbit anti-PLOD2 antibodies (1:300; 21214-1-AP; Proteintech Group, Inc., Chicago, IL, USA). Anti-GAPDH antibodies (1:1,000; ab8245; Abcam) were used as an internal loading control. The membranes were washed and incubated with anti-rabbit IgG horseradish peroxidase (HRP)-linked antibodies (#7074; Cell Signaling Technology). Complexes were visualized with Clarity Western Substrate (Bio-Rad Laboratories).

Screening of *miR-26a* and *miR-26b* target genes using *in silico* analysis and gene expression data. To identify *miR-26a/b* target genes, we used *in silico* analysis and genome-wide gene expression analysis. First, we screened genes using TargetScan release 6.2 (<http://www.targetscan.org/>). Next, to identify upregulated genes in ccRCC clinical specimens, we analyzed publicly available gene expression profiles in the GEO database (accession nos. GSE22541 and GSE36895). Our strategies for miRNA target screening were previously described (12,20,21).

Plasmid construction and dual-luciferase reporter assay. Partial wild-type sequences of the *LOXL2* and *PLOD2* 3'-untranslated region (UTR) or those with deleted *miR-26a/b* binding sites were inserted between the *XhoI-PmeI* restriction

sites in the 3'-UTR of the *hRluc* gene in the psiCHECK-2 vector (C8021; Promega, Madison, WI, USA). The procedure for the dual-luciferase reporter assay was previously described (12,20,21).

Statistical analysis. The relationships between the two groups and the numerical values obtained by real-time RT-PCR were analyzed using the Mann-Whitney U-test. The relationships among the three variables and numerical values were analyzed using the Bonferroni-adjusted Mann-Whitney U test. Spearman's rank test was used to evaluate the correlations between the expression of (*miR-26a* and *LOXL2*), (*miR-26a* and *PLOD2*), (*miR-26b* and *LOXL2*) and (*miR-26b* and *PLOD2*). All analyses were performed using Expert StatView (version 5; SAS Institute, Inc., Cary, NC, USA).

Results

Expression levels of *miR-26a* and *miR-26b* in ccRCC clinical specimens and cell lines. The expression levels of *miR-26a* and *miR-26b* were significantly lower in ccRCC specimens than in corresponding non-cancerous specimens ($P=0.0171$ and $P=0.0136$, respectively; Fig. 1A and B). In 786-O and A498 cells, the expression levels of *miR-26a* or *miR-26b* were lower than in non-cancerous specimens.

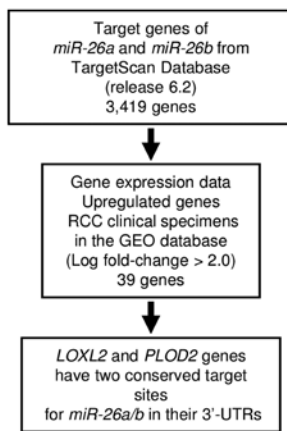


Figure 2. Strategy for selecting target genes regulated by *miR-26a* and *miR-26b* in RCC cells.

Effects of *miR-26a* and *miR-26b* restoration on cell proliferation, migration and invasion activities in ccRCC cells. To investigate the functional effects of *miR-26a* or *miR-26b*, we performed gain-of-function studies using mature miRNA transfection of 786-O and A498 cells.

The XTT assays demonstrated that cell proliferation was not inhibited in *miR-26a* or *miR-26b* transfectants in comparison with the mock or miR-control transfectants (Fig. 1C).

In contrast, the migration assays demonstrated that cell migration activity was significantly inhibited in *miR-26a* or *miR-26b* transfectant cells in comparison with the mock or miR-control transfectants (Fig. 1D). The Matrigel invasion assays demonstrated that cell invasion activity was significantly inhibited in *miR-26a* or *miR-26b* transfectant cells in comparison with the mock or miR-control transfectants (Fig. 1E).

Identification of candidate target genes of *miR-26a* and *miR-26b* in ccRCC cells. To identify target genes of *miR-26a* and *miR-26b* (the seed sequences of the two miRNAs are identical), we used *in silico* analysis and genome-wide gene expression data. First, we searched the TargetScan database (release 6.2: <http://www.targetscan.org/>) and identified 3,419 genes that had putative target sites for *miR-26a* and *miR-26b* in their 3'-UTRs. Next, we pared down the list of putative candidate genes based on upregulated genes determined by the gene expression data set of RCC clinical specimens in the GEO (Gene Expression Omnibus) database (accession numbers: GSE36895, GSE22541). The flow chart outlining our strategy for identification of candidate target genes of *miR-26a* and *miR-26b* is shown in Fig. 2.

From this selection, 39 candidate genes were identified as targets of *miR-26a* and *miR-26b* (Table II). Among these candidate genes, we focused on *LOXL2* and *PLOD2* genes because these genes have two conserved target sites for *miR-26a* and *miR-26b* in their 3'-UTRs, and function as collagen cross-linking enzymes associated with extracellular matrix (ECM) stiffness. Recent studies showed that aberrantly expressed ECM contributes to cancer cell metastasis (22,23). Therefore, these two genes were chosen for further analysis.

Direct regulation of *LOXL2* and *PLOD2* by *miR-26a* and *miR-26b* in ccRCC cells. We first performed qRT-PCR and Western blotting to investigate whether expression of the *LOXL2* gene and protein were reduced by restoration of *miR-26a* or *miR-26b* in 786-O and A498 cells. We found that the mRNA and protein expression levels of *LOXL2*/LOXL2 were significantly repressed in *miR-26a* or *miR-26b* transfectant cells in comparison with mock or miR-control transfectants (Fig. 3A and B).

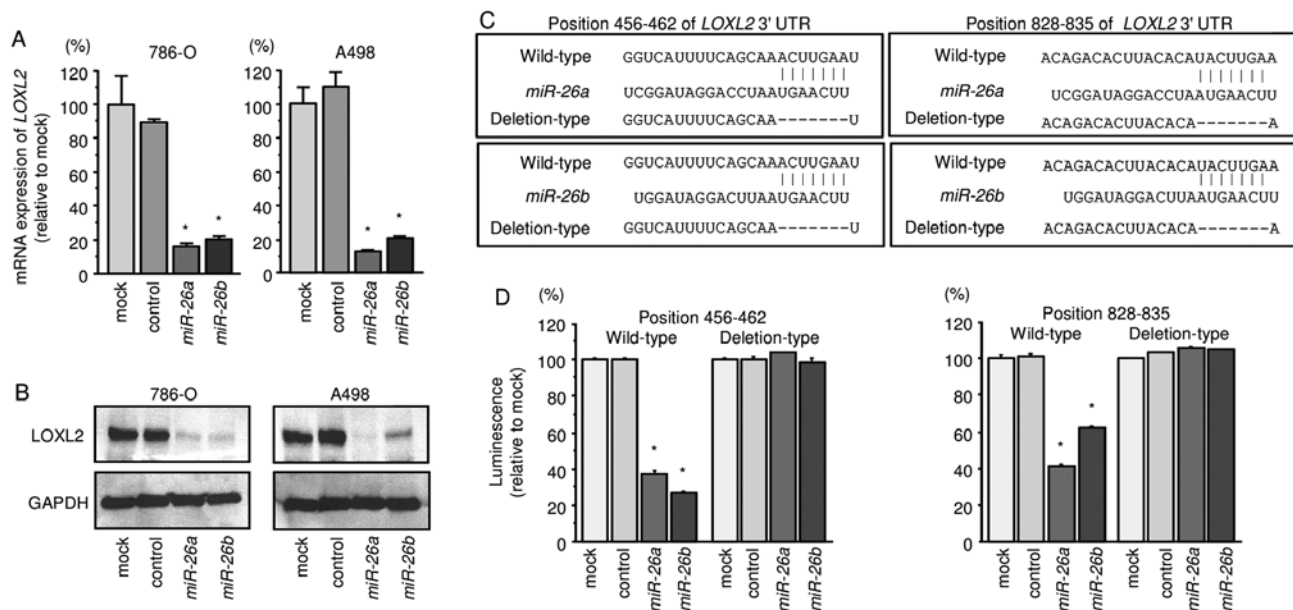


Figure 3. Expression of the gene encoding *LOXL2* is suppressed by transfection of RCC cell lines 786-O and A498 with *miR-26a* or *miR-26b*. (A) *LOXL2* mRNA expression was evaluated by quantitative RT-PCR 72 h after transfection with *miR-26a* or *miR-26b* (10 nM). *GUSB* was used as an internal control. * $P < 0.01$. (B) *LOXL2* protein expression was evaluated by western blotting 72 h after transfection with *miR-26a* or *miR-26b* (10 nM). GAPDH was used as a loading control. (C) *miR-26a* and *miR-26b* binding sites in the 3'-UTR of *LOXL2* mRNA. (D) Luciferase reporter assays in A498 cells using vectors encoding putative *miR-26a* and *miR-26b* target sites at position 456-462 and 828-835 of the *LOXL2* 3'-UTR. *Renilla* luciferase values were normalized to firefly luciferase values. * $P < 0.0001$.

Table II. Putative candidate target genes regulated by *miR-26a* and *miR-26b* in RCC cells.

Entrez gene ID	Symbol	Gene name	Location	No. of conserved target sites	No. of poorly conserved target sites	GEO (GSE36895, GSE22541) average fold-change
5352	<i>PLOD2</i>	Procollagen-lysine, 2-oxoglutarate 5-dioxygenase 2	3q24	2	0	2.2220507
4017	<i>LOXL2</i>	Lysyl oxidase-like 2	8p21.3	2	0	2.7719142
2146	<i>EZH2</i>	Enhancer of zeste homolog 2 (<i>Drosophila</i>)	7q35-q36	1	0	2.0032272
3625	<i>INHBB</i>	Inhibin, β B	2cen-q13	1	0	3.7558112
3678	<i>ITGA5</i>	Integrin, α 5 (fibronectin receptor, α polypeptide)	12q11-q13	1	0	2.8391342
23023	<i>TMCC1</i>	Transmembrane and coiled-coil domain family 1	3q22.1	1	1	2.226072
1404	<i>HAPLN1</i>	Hyaluronan and proteoglycan link protein 1	5q14.3	1	1	2.7813237
7903	<i>ST8SIA4</i>	ST8 α -N-acetyl-neuraminide α -2,8-sialyltransferase 4	5q21	1	0	3.1741676
1846	<i>DUSP4</i>	Dual specificity phosphatase 4	8p12-p11	1	0	2.1518986
6890	<i>TAP1</i>	Transporter 1, ATP-binding cassette, sub-family B (MDR/TAP)	6p21.3	0	1	2.0403051
7272	<i>TTK</i>	TTK protein kinase	6q14.1	0	1	2.3837836
170384	<i>FUT11</i>	Fucosyltransferase 11 (α (1,3) fucosyltransferase)	10q22.2	0	1	2.0443428
22974	<i>TPX2</i>	TPX2, microtubule-associated, homolog (<i>Xenopus laevis</i>)	20q11.2	0	1	2.662108
2210	<i>FCGR1B</i>	Fc fragment of IgG, high affinity Ib, receptor (CD64)	1p11.2	0	1	2.294377
4747	<i>NEFL</i>	Neurofilament, light polypeptide	8p21	0	1	2.1319628
5836	<i>PYGL</i>	Phosphorylase, glycogen, liver	14q21-q22	0	1	2.0643747
1234	<i>CCR5</i>	Chemokine (C-C motif) receptor 5	3p21.31	0	1	3.3846455
55165	<i>CEP55</i>	Centrosomal protein 55 kDa	10q23.33	0	1	2.0711598
10288	<i>LILRB2</i>	Leukocyte immunoglobulin-like receptor, subfamily B (with TM and ITIM domains), member 2	19q13.4	0	1	2.454539
1356	<i>CP</i>	Ceruloplasmin (ferroxidase)	3q23-q25	0	1	3.9467278
3910	<i>LAMA4</i>	Laminin, α 4	6q21	0	1	2.2182174
163404	<i>LPPR5</i>	Lipid phosphate phosphatase-related protein type 5	1p21.3	0	1	2.450066
5027	<i>P2RX7</i>	Purinergic receptor P2X, ligand-gated ion channel, 7	12q24	0	3	3.0084689
330	<i>BIRC3</i>	Baculoviral IAP repeat containing 3	11q22	0	1	2.2927191
6507	<i>SLC1A3</i>	Solute carrier family 1 (glial high affinity glutamate transporter), member 3	5p13	0	1	2.1052346
2335	<i>FNI</i>	Fibronectin 1	2q34	0	1	2.4469628
8701	<i>DNAH11</i>	Dynein, axonemal, heavy chain 11	7p21	0	1	2.2785249
79850	<i>FAM57A</i>	Family with sequence similarity 57, member A	17p13.3	0	1	2.2900116
1462	<i>VCAN</i>	Versican	5q14.3	0	1	2.524361
128346	<i>C1orf162</i>	Chromosome 1 open reading frame 162	1p13.2	0	1	2.2255776
4015	<i>LOX</i>	Lysyl oxidase	5q23.2	0	1	3.3194032
115761	<i>ARL11</i>	ADP-ribosylation factor-like 11	13q14.2	0	1	2.4013827
286336	<i>FAM78A</i>	Family with sequence similarity 78, member A	9q34	0	1	2.1942985
6664	<i>SOX11</i>	SRY (sex determining region Y)-box 11	2p25	0	1	2.577679
9770	<i>RASSF2</i>	Ras association (RalGDS/AF-6) domain family member 2	20p13	0	1	2.619857
57823	<i>SLAMF7</i>	SLAM family member 7	1q23.1-q24.1	0	1	2.063896
58475	<i>MS4A7</i>	Membrane-spanning 4-domains, subfamily A, member 7	11q12	0	1	2.0315962
79742	<i>CXorf36</i>	Chromosome X open reading frame 36	Xp11.3	0	1	2.3148956
146857	<i>SLFN13</i>	Schlafen family member 13	17q12	0	1	2.6972997

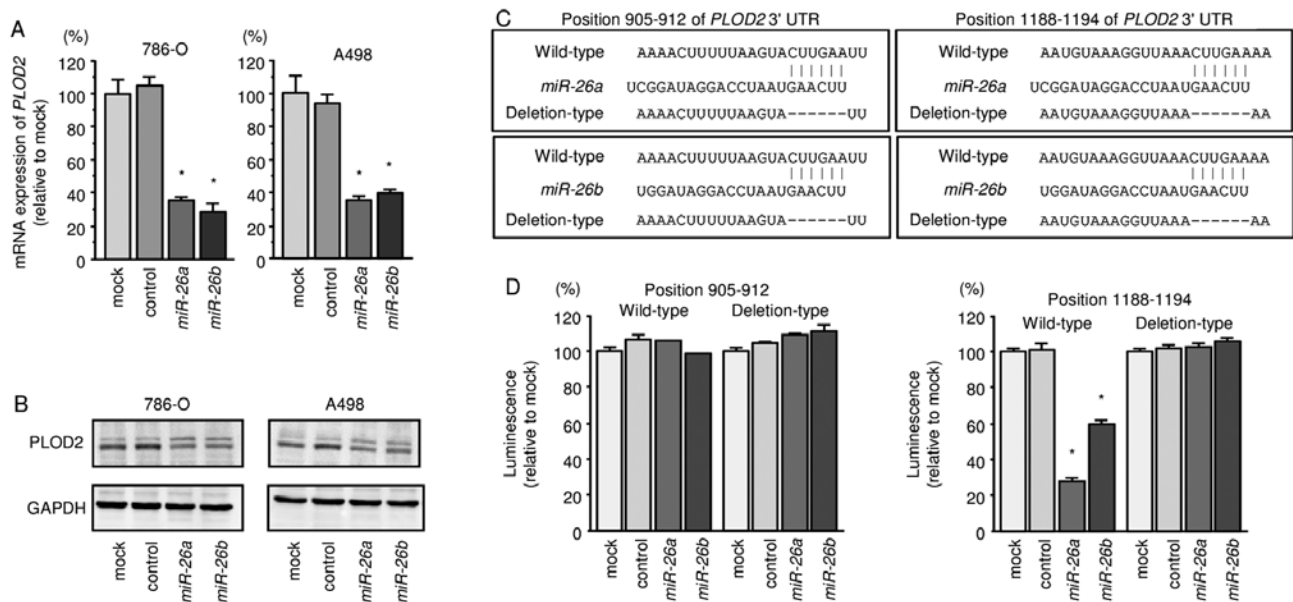


Figure 4. Expression of the gene encoding *PLOD2* is suppressed by transfection of RCC cell lines 786-O and A498 with *miR-26a* or *miR-26b*. (A) *PLOD2* mRNA expression was evaluated by quantitative RT-PCR 72 h after transfection with *miR-26a* or *miR-26b* (10 nM). *GUSB* was used as an internal control. * $P < 0.01$. (B) *PLOD2* protein expression was evaluated by western blotting 72 h after transfection with *miR-26a* or *miR-26b* (10 nM). *GAPDH* was used as a loading control. (C) *miR-26a* and *miR-26b* binding site in the 3'-UTR of *PLOD2* mRNA. (D) Luciferase reporter assays in A498 cells using a vector encoding a putative *miR-26a* and *miR-26b* target sites at position 905-912 and 1188-1194 of the *PLOD2* 3'-UTR. *Renilla* luciferase values were normalized to firefly luciferase values. * $P < 0.0001$.

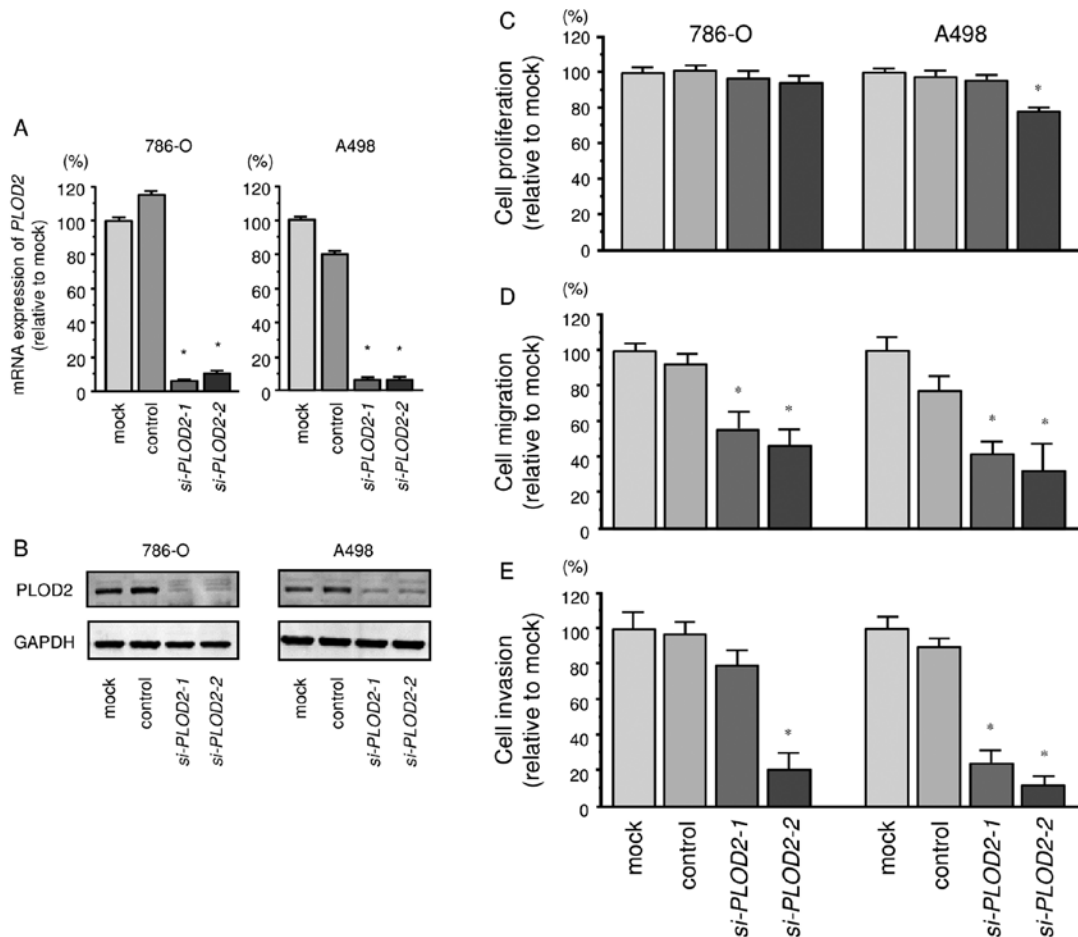


Figure 5. Effects on RCC cell proliferation, migration and invasion after silencing of *PLOD2* mRNA and protein expression with *si-PLOD2* transfection. (A) *PLOD2* mRNA expression levels were evaluated by quantitative RT-PCR 72 h after transfection with *si-PLOD2* (10 nM). *GUSB* was used as an internal control. * $P < 0.0001$. (B) *PLOD2* protein expression levels were evaluated by western blotting 72 h after transfection with *si-PLOD2* (10 nM). *GAPDH* was used as a loading control. (C) Cell proliferation was determined by XTT assays. (D) Cell migration activity was determined by wound-healing assays. (E) Cell invasion activity was determined by Matrigel invasion assays. * $P < 0.0001$.

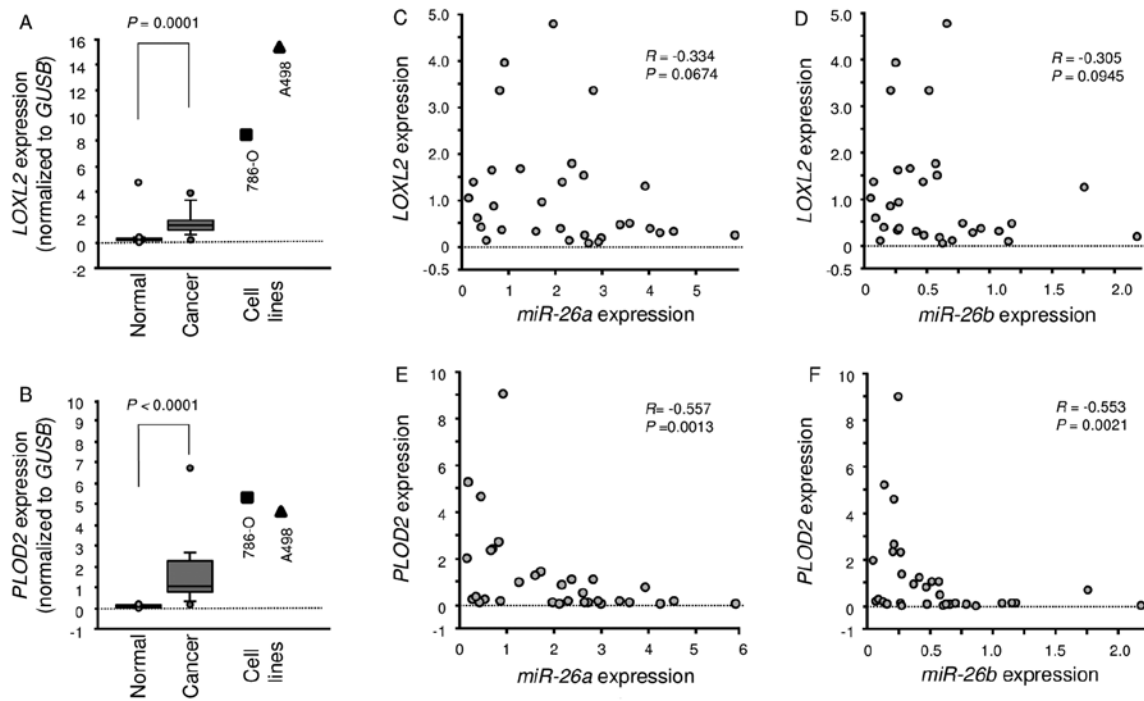


Figure 6. Expression levels of *LOXL2* and *PLOD2* in ccRCC clinical specimens and cell lines 786-O and A498. (A and B) Quantitative real-time RT-PCR showed that the expression levels of *LOXL2* and *PLOD2* were significantly higher in ccRCC tissues and RCC cell lines than in normal kidney tissues. *GUSB* was used as an internal control. (C and D) Correlations between *LOXL2*-*miR-26a* expression or *LOXL2*-*miR-26b* expression were determined in RCC clinical specimens. (E and F) Correlations between *PLOD2*-*miR-26a* expression or *PLOD2*-*miR-26b* expression were determined in RCC clinical specimens.

Next, to investigate whether *LOXL2* mRNA had target sites for *miR-26a* or *miR-26b*, we performed luciferase reporter assays in 786-O cells. We used vectors encoding either the partial wild-type sequence of the 3'-UTR of *LOXL2*, including the predicted *miR-26a/b* target sites, or deletion vectors lacking the *miR-26a/b* target sites. We found that the luminescence intensities were significantly reduced by transfection with *miR-26a* or *miR-26b* and vectors carrying the wild-type 3'-UTR of *LOXL2*, whereas transfection with deletion vectors blocked the decrease in luminescence. These data suggested that *miR-26a* or *miR-26b* bound directly to specific sites in the 3'-UTR of *LOXL2* (Fig. 3C and D).

We also found that the mRNA and protein expression levels of *PLOD2*/*PLOD2* were significantly repressed in *miR-26a* or *miR-26b* transfectant cells in comparison with mock or miR-control transfectants (Fig. 4A and B). We also observed that the luminescence intensities were significantly reduced by transfection with *miR-26a* or *miR-26b* and vectors carrying the wild-type 3'-UTR of *PLOD2*, whereas transfection with deletion vectors blocked the decrease in luminescence. These data suggested that *miR-26a* or *miR-26b* bound directly to specific sites in the 3'-UTR of *PLOD2* (Fig. 4C and D).

Silencing *PLOD2* affected cell proliferation, migration and invasion activities in ccRCC cells. We recently presented a loss-of-function study of *LOXL2* in RCC cells (786-O and A498) by using two siRNAs (786-O and A498) (12). Those data showed that the silencing of *LOXL2* significantly suppressed cancer cell migration and invasion activities in RCC cells.

To investigate the functional role of *PLOD2* in ccRCC cells, we performed a loss-of-function study using *si-PLOD2* transfected cells. First, we evaluated the knockdown efficiency

of *si-PLOD2* transfection in 786-O and A498 cells. qRT-PCR and western blotting indicated that *si-PLOD2* transfection effectively downregulated *PLOD2* expression in both cell lines (786-O, $P < 0.0001$; A498, $P < 0.0001$; Fig. 5A and B).

The XTT assay demonstrated that cell proliferation was not inhibited significantly in *si-PLOD2* transfectant cells in comparison with the mock or negative control transfectants (Fig. 5C).

In contrast, the migration assay demonstrated that cell migration activity was significantly inhibited in *si-PLOD2* transfectants in comparison with the mock or negative control transfectants (Fig. 5D). The Matrigel invasion assay demonstrated that invasive activity was significantly inhibited in *si-PLOD2* transfectants in comparison with the mock or negative control transfectants (Fig. 5E).

Expression of *LOXL2* and *PLOD2* in ccRCC clinical specimens. A total of 15 pairs of ccRCC specimens and corresponding non-cancerous specimens were used for expression studies of *LOXL2* and *PLOD2* using RT-PCR. We showed that *LOXL2* and *PLOD2* were significantly upregulated in cancer tissues compared with normal tissues ($P = 0.0001$ and $P < 0.0001$, respectively; Fig. 6A and B). Furthermore, Spearman's rank test showed a negative correlation between the expression of *miR-26a*/*PLOD2* and *miR-26b*/*PLOD2* (Fig. 6E and F).

Discussion

A growing body of evidence has shown that aberrantly expressed miRNAs can disrupt tightly regulated RNA networks in cancer cells and promote human oncogenesis and metastasis (7,9,24-26). Recently, our studies identified a

variety of novel RCC molecular pathways regulated by tumor-suppressive miRNAs (12-15). In the present study, we focused on *miR-26a* and *miR-26b* because the expression levels of these miRNAs were reduced in the miRNA signatures of various types of cancers (10,18,19,27). Moreover, the functional roles of these miRNAs in RCC cells are not clear. Our present data showed that *miR-26a* and *miR-26b* act as tumor suppressors that modulate cancer cell migration and invasion in RCC cells. Our previous studies of oral cancer and prostate cancer demonstrated the tumor-suppressive roles of these miRNAs (19,20), and those findings support the present results obtained with RCC cells. Downregulation and tumor-suppressive roles of *miR-26a* or *miR-26b* have been reported in several types of cancer, such as bladder, breast, hepatocellular carcinoma and oral cancer (19,28-30).

In the human genome, the *miR-26* family consists of three subtypes of miRNAs: *miR-26a-1*, *miR-26a-2* and *miR-26b*. The mature sequences of *miR-26a-1* and *miR-26a-2* are identical, whereas the two nucleotides differ from that of *miR-26b* (miRBase release 21; <http://www.mirbase.org/>). The molecular mechanisms responsible for silencing the expression of the *miR-26* family are still unclear. A recent study indicated that *MYC* oncogene directly bound to the promoter regions of *miR-26a-1*, *miR-26a-2* and *miR-26b* and negatively regulated expression of these miRNAs in prostate cancer cells (31). Overexpression of *MYC* was observed in RCC clinical specimens (15,32), suggesting *MYC* might be a mediator for expression control of tumor-suppressive miRNAs in cancer cells.

A single miRNA may regulate multiple protein-coding genes; indeed, bioinformatics studies have shown that miRNAs regulate >30-60% of the protein-coding genes in the human genome (7,33). Reduced expression of tumor-suppressive miRNAs may cause overexpression of oncogenic genes in cancer cells. To better understand RCC oncogenesis and metastasis, we identified *miR-26a* and *miR-26b* target genes using *in silico* analysis. Recent miRNA studies in our laboratory have utilized this strategy to identify novel molecular targets and pathways regulated by tumor-suppressive miRNAs in several cancers, including RCC (12,20).

A total of 39 putative target genes of *miR-26a* and *miR-26b* were identified in the present study. Among these genes, we focused on *LOXL2* and *PLOD2* because they function as collagen cross-linking enzymes. Numerous studies have shown that aberrant expression of collagen cross-linking enzymes promotes extracellular matrix (ECM) stiffening, resulting in enhanced cancer cell migration and invasion (22,34-39). Overexpression of ECM components has been observed in several cancers (21,23,40). Recently, a number of studies indicated that several miRNAs regulated ECM component genes, and aberrantly expressed miRNAs have contributed to cancer cell progression by dysregulation of cell adhesion, polarity and ECM remodeling (21,23). Our past studies found that the tumor-suppressive *miR-29*-family (*miR-29a*, *miR-29b* and *miR-29c*) and *miR-218* directly regulated laminins (*LAMC2* and *LAMB3*) and integrins (*ITGA6* and *ITGB3*), such that restoration of these miRNAs inhibited cancer cell migration and invasion (21,41,42).

Once collagen is secreted, collagen cross-linking occurs on lysine and hydroxylysine residues by the lysyl oxidase (LOX)

family of enzymes (22,43). More recently, we showed that the *miR-29s*-family directly targeted *LOXL2* in RCC and lung cancers (12). Overexpression of *LOXL2* was observed in RCC clinical specimens and silencing of *LOXL2* inhibited cancer cell migration and invasion in ccRCC cell lines (12). Other research groups found that increased expression of *LOXL2* is correlated with disease progression, including RCC (34,44). The function of the LOX-family is covalent crosslinking of collagen and/or elastin in the ECM (35,36). Aberrant expression of LOX-family proteins has been reported in several diseases, including cancers (34-39). Interestingly, *LOXL2* is a direct transcriptional target of HIF-1. Moreover, nuclear *LOXL2* interacts with transcription factor SNAIL1 and represses E-cadherin as well as induces EMT (45,46). In this study, we demonstrated direct regulation of *LOXL2* by *miR-26a* and *miR-26b* in RCC cells as observed with the *miR-29s*-family. These findings showed that tumor-suppressive *miR-26a/b*-*LOXL2* is the pivotal pathway contributing to cancer cell migration and invasion in RCC.

In this study, we also focused on the *PLOD2* (procollagen-lysine 2-oxyglutarate-dioxygenase) gene as a target of *miR-26a* and *miR-26b* and demonstrated the direct regulation of these miRNAs by luciferase reporter assays. *PLOD2* encodes an enzyme that mediates collagen lysine hydroxylation. Collagen cross-linking that are derived from hydroxylated lysine residues have increased stability compared with non-hydroxylated lysine residues (22,47). Overexpression of *PLOD2* in ccRCC clinical specimens and promoting migration and invasion in cancer cells were observed in the present study. In breast cancer, Kaplan-Meier curves of disease-specific survival stratified by *PLOD2* expression revealed that high *PLOD2* expression was significantly associated with decreased disease-specific survival (48). Moreover, *PLOD2* expression promoted tumor stiffness and was required for metastasis to lymph nodes and lungs (22,48).

In conclusion, *miR-26a* and *miR-26b* were significantly downregulated in ccRCC clinical specimens and appeared to function as tumor suppressors through regulation of collagen cross-linking enzymes, *LOXL2* and *PLOD2*, both of which function as oncogenes in this disease. The identification of novel molecular targets and pathways regulated by the tumor-suppressive *miR-26a* and *miR-26b* may lead to a better understanding of ccRCC and the development of new therapeutic strategies to treat this disease.

Acknowledgements

The present study was supported by the Japanese Society for the Promotion of Science (KAKENHI), grant numbers (C) 15K10801, (C) 15K20070, (C) 15K20071, and (B) 25293333.

References

1. Rini BI, Campbell SC and Escudier B: Renal cell carcinoma. *Lancet* 373: 1119-1132, 2009.
2. Randall JM, Millard F and Kurzrock R: Molecular aberrations, targeted therapy, and renal cell carcinoma: Current state-of-the-art. *Cancer Metastasis Rev* 33: 1109-1124, 2014.
3. Gupta K, Miller JD, Li JZ, Russell MW and Charbonneau C: Epidemiologic and socioeconomic burden of metastatic renal cell carcinoma (mRCC): A literature review. *Cancer Treat Rev* 34: 193-205, 2008.

4. Motzer RJ and Russo P: Systemic therapy for renal cell carcinoma. *J Urol* 163: 408-417, 2000.
5. Motzer RJ, Hutson TE, Tomczak P, Michaelson MD, Bukowski RM, Oudard S, Negrier S, Szczylik C, Pili R, Bjarnason GA, *et al*: Overall survival and updated results for sunitinib compared with interferon alfa in patients with metastatic renal cell carcinoma. *J Clin Oncol* 27: 3584-3590, 2009.
6. Motzer RJ, Hutson TE, Tomczak P, Michaelson MD, Bukowski RM, Rixe O, Oudard S, Negrier S, Szczylik C, Kim ST, *et al*: Sunitinib versus interferon alfa in metastatic renal-cell carcinoma. *N Engl J Med* 356: 115-124, 2007.
7. Filipowicz W, Bhattacharyya SN and Sonenberg N: Mechanisms of post-transcriptional regulation by microRNAs: Are the answers in sight? *Nat Rev Genet* 9: 102-114, 2008.
8. Bartel DP: MicroRNAs: Genomics, biogenesis, mechanism, and function. *Cell* 116: 281-297, 2004.
9. Nelson KM and Weiss GJ: MicroRNAs and cancer: Past, present, and potential future. *Mol Cancer Ther* 7: 3655-3660, 2008.
10. Goto Y, Kurozumi A, Enokida H, Ichikawa T and Seki N: Functional significance of aberrantly expressed microRNAs in prostate cancer. *Int J Urol* 22: 242-252, 2015.
11. Esquela-Kerscher A and Slack FJ: Oncomirs - microRNAs with a role in cancer. *Nat Rev Cancer* 6: 259-269, 2006.
12. Nishikawa R, Chiyomaru T, Enokida H, Inoguchi S, Ishihara T, Matsushita R, Goto Y, Fukumoto I, Nakagawa M and Seki N: Tumour-suppressive microRNA-29s directly regulate LOXL2 expression and inhibit cancer cell migration and invasion in renal cell carcinoma. *FEBS Lett* 589: 2136-2145, 2015.
13. Yamasaki T, Seki N, Yoshino H, Itesako T, Hidaka H, Yamada Y, Tatarano S, Yonezawa T, Kinoshita T, Nakagawa M, *et al*: MicroRNA-218 inhibits cell migration and invasion in renal cell carcinoma through targeting caveolin-2 involved in focal adhesion pathway. *J Urol* 190: 1059-1068, 2013.
14. Yoshino H, Enokida H, Itesako T, Tatarano S, Kinoshita T, Fuse M, Kojima S, Nakagawa M and Seki N: Epithelial-mesenchymal transition-related microRNA-200s regulate molecular targets and pathways in renal cell carcinoma. *J Hum Genet* 58: 508-516, 2013.
15. Yamada Y, Hidaka H, Seki N, Yoshino H, Yamasaki T, Itesako T, Nakagawa M and Enokida H: Tumor-suppressive microRNA-135a inhibits cancer cell proliferation by targeting the c-MYC oncogene in renal cell carcinoma. *Cancer Sci* 104: 304-312, 2013.
16. Yoshino H, Enokida H, Itesako T, Kojima S, Kinoshita T, Tatarano S, Chiyomaru T, Nakagawa M and Seki N: Tumor-suppressive microRNA-143/145 cluster targets hexokinase-2 in renal cell carcinoma. *Cancer Sci* 104: 1567-1574, 2013.
17. Ishihara T, Seki N, Inoguchi S, Yoshino H, Tatarano S, Yamada Y, Itesako T, Goto Y, Nishikawa R, Nakagawa M, *et al*: Expression of the tumor suppressive miRNA-23b/27b cluster is a good prognostic marker in clear cell renal cell carcinoma. *J Urol* 192: 1822-1830, 2014.
18. Kikkawa N, Hanazawa T, Fujimura L, Nohata N, Suzuki H, Chazono H, Sakurai D, Horiguchi S, Okamoto Y and Seki N: miR-489 is a tumour-suppressive miRNA target PTPN11 in hypopharyngeal squamous cell carcinoma (HSCC). *Br J Cancer* 103: 877-884, 2010.
19. Fukumoto I, Hanazawa T, Kinoshita T, Kikkawa N, Koshizuka K, Goto Y, Nishikawa R, Chiyomaru T, Enokida H, Nakagawa M, *et al*: MicroRNA expression signature of oral squamous cell carcinoma: Functional role of microRNA-26a/b in the modulation of novel cancer pathways. *Br J Cancer* 112: 891-900, 2015.
20. Kato M, Goto Y, Matsushita R, Kurozumi A, Fukumoto I, Nishikawa R, Sakamoto S, Enokida H, Nakagawa M, Ichikawa T, *et al*: MicroRNA-26a/b directly regulate La-related protein 1 and inhibit cancer cell invasion in prostate cancer. *Int J Oncol* 47: 710-718, 2015.
21. Kinoshita T, Hanazawa T, Nohata N, Kikkawa N, Enokida H, Yoshino H, Yamasaki T, Hidaka H, Nakagawa M, Okamoto Y, *et al*: Tumor suppressive microRNA-218 inhibits cancer cell migration and invasion through targeting laminin-332 in head and neck squamous cell carcinoma. *Oncotarget* 3: 1386-1400, 2012.
22. Gilkes DM, Semenza GL and Wirtz D: Hypoxia and the extracellular matrix: Drivers of tumour metastasis. *Nat Rev Cancer* 14: 430-439, 2014.
23. Kurozumi A, Goto Y, Matsushita R, Fukumoto I, Kato M, Nishikawa R, Sakamoto S, Enokida H, Nakagawa M, Ichikawa T, *et al*: Tumor-suppressive microRNA-223 inhibits cancer cell migration and invasion by targeting ITGA3/ITGB1 signaling in prostate cancer. *Cancer Sci* 107: 84-94, 2015.
24. Wiemer EA: The role of microRNAs in cancer: No small matter. *Eur J Cancer* 43: 1529-1544, 2007.
25. Singh SK, Pal Bhadra M, Girschick HJ and Bhadra U: MicroRNAs - micro in size but macro in function. *FEBS J* 275: 4929-4944, 2008.
26. Iorio MV and Croce CM: MicroRNAs in cancer: Small molecules with a huge impact. *J Clin Oncol* 27: 5848-5856, 2009.
27. Fuse M, Kojima S, Enokida H, Chiyomaru T, Yoshino H, Nohata N, Kinoshita T, Sakamoto S, Naya Y, Nakagawa M, *et al*: Tumor suppressive microRNAs (miR-222 and miR-31) regulate molecular pathways based on microRNA expression signature in prostate cancer. *J Hum Genet* 57: 691-699, 2012.
28. Lin Y, Chen H, Hu Z, Mao Y, Xu X, Zhu Y, Xu X, Wu J, Li S, Mao Q, *et al*: miR-26a inhibits proliferation and motility in bladder cancer by targeting HMGAI. *FEBS Lett* 587: 2467-2473, 2013.
29. Zhang B, Liu XX, He JR, Zhou CX, Guo M, He M, Li MF, Chen GQ and Zhao Q: Pathologically decreased miR-26a antagonizes apoptosis and facilitates carcinogenesis by targeting MTDH and EZH2 in breast cancer. *Carcinogenesis* 32: 2-9, 2011.
30. Zhu Y, Lu Y, Zhang Q, Liu JJ, Li TJ, Yang JR, Zeng C and Zhuang SM: MicroRNA-26a/b and their host genes cooperate to inhibit the G1/S transition by activating the pRb protein. *Nucleic Acids Res* 40: 4615-4625, 2012.
31. Koh CM, Iwata T, Zheng Q, Bethel C, Yegnasubramanian S and De Marzo AM: Myc enforces overexpression of EZH2 in early prostatic neoplasia via transcriptional and post-transcriptional mechanisms. *Oncotarget* 2: 669-683, 2011.
32. Tang SW, Chang WH, Su YC, Chen YC, Lai YH, Wu PT, Hsu CI, Lin WC, Lai MK and Lin JY: MYC pathway is activated in clear cell renal cell carcinoma and essential for proliferation of clear cell renal cell carcinoma cells. *Cancer Lett* 273: 35-43, 2009.
33. Friedman RC, Farh KK, Burge CB and Bartel DP: Most mammalian mRNAs are conserved targets of microRNAs. *Genome Res* 19: 92-105, 2009.
34. Barker HE, Cox TR and Erler JT: The rationale for targeting the LOX family in cancer. *Nat Rev Cancer* 12: 540-552, 2012.
35. Kagan HM and Li W: Lysyl oxidase: Properties, specificity, and biological roles inside and outside of the cell. *J Cell Biochem* 88: 660-672, 2003.
36. Vadasz Z, Kessler O, Akiri G, Gengrinovitch S, Kagan HM, Baruch Y, Izhak OB and Neufeld G: Abnormal deposition of collagen around hepatocytes in Wilson's disease is associated with hepatocyte specific expression of lysyl oxidase and lysyl oxidase like protein-2. *J Hepatol* 43: 499-507, 2005.
37. Kim YM, Kim EC and Kim Y: The human lysyl oxidase-like 2 protein functions as an amine oxidase toward collagen and elastin. *Mol Biol Rep* 38: 145-149, 2011.
38. Fong SF, Dietzsch E, Fong KS, Hollosi P, Asuncion L, He Q, Parker MI and Csiszar K: Lysyl oxidase-like 2 expression is increased in colon and esophageal tumors and associated with less differentiated colon tumors. *Genes Chromosomes Cancer* 46: 644-655, 2007.
39. Peinado H, Moreno-Bueno G, Hardisson D, Pérez-Gómez E, Santos V, Mendiola M, de Diego JI, Nistal M, Quintanilla M, Portillo F, *et al*: Lysyl oxidase-like 2 as a new poor prognosis marker of squamous cell carcinomas. *Cancer Res* 68: 4541-4550, 2008.
40. Liu LX, Jiang HC, Liu ZH, Zhou J, Zhang WH, Zhu AL, Wang XQ and Wu M: Integrin gene expression profiles of human hepatocellular carcinoma. *World J Gastroenterol* 8: 631-637, 2002.
41. Kinoshita T, Nohata N, Hanazawa T, Kikkawa N, Yamamoto N, Yoshino H, Itesako T, Enokida H, Nakagawa M, Okamoto Y, *et al*: Tumour-suppressive microRNA-29s inhibit cancer cell migration and invasion by targeting laminin-integrin signalling in head and neck squamous cell carcinoma. *Br J Cancer* 109: 2636-2645, 2013.
42. Yamamoto N, Kinoshita T, Nohata N, Itesako T, Yoshino H, Enokida H, Nakagawa M, Shozu M and Seki N: Tumor suppressive microRNA-218 inhibits cancer cell migration and invasion by targeting focal adhesion pathways in cervical squamous cell carcinoma. *Int J Oncol* 42: 1523-1532, 2013.

43. Gordon MK and Hahn RA: Collagens. *Cell Tissue Res* 339: 247-257, 2010.
44. Hase H, Jingushi K, Ueda Y, Kitae K, Egawa H, Ohshio I, Kawakami R, Kashiwagi Y, Tsukada Y, Kobayashi T, *et al*: *LOXL2* status correlates with tumor stage and regulates integrin levels to promote tumor progression in ccRCC. *Mol Cancer Res* 12: 1807-1817, 2014.
45. Schietke R, Warnecke C, Wacker I, Schödel J, Mole DR, Campean V, Amann K, Goppelt-Strube M, Behrens J, Eckardt KU, *et al*: The lysyl oxidases LOX and LOXL2 are necessary and sufficient to repress E-cadherin in hypoxia: Insights into cellular transformation processes mediated by HIF-1. *J Biol Chem* 285: 6658-6669, 2010.
46. Moon HJ, Finney J, Xu L, Moore D, Welch DR and Mure M: MCF-7 cells expressing nuclear associated lysyl oxidase-like 2 (*LOXL2*) exhibit an epithelial-to-mesenchymal transition (EMT) phenotype and are highly invasive in vitro. *J Biol Chem* 288: 30000-30008, 2013.
47. van der Slot AJ, Zuurmond AM, van den Bogaerdt AJ, Ulrich MM, Middelkoop E, Boers W, Karel Runday H, DeGroot J, Huizinga TW and Bank RA: Increased formation of pyridinoline cross-links due to higher telopeptide lysyl hydroxylase levels is a general fibrotic phenomenon. *Matrix Biol* 23: 251-257, 2004.
48. Gilkes DM, Bajpai S, Wong CC, Chaturvedi P, Hubbi ME, Wirtz D and Semenza GL: Procollagen lysyl hydroxylase 2 is essential for hypoxia-induced breast cancer metastasis. *Mol Cancer Res* 11: 456-466, 2013.